NLR MP 85050 U

NATIONAAL LUCHT- EN RUIMTEVAARTLABORATORIUM

NATIONAL AEROSPACE LABORATORY NLR

THE NETHERLANDS

NLR MP 85050 U

FATIGUE FRACTURE IN STEEL LANDING GEAR COMPONENTS

BY

R.J.H. WANHILL

NLR MP 85050 U

FATIGUE FRACTURE IN STEEL LANDING GEAR COMPONENTS

by

R.J.H. Wanhill

(11 pages in total)

Division: Structures and Materials
Prepared: RJHW/
Approved: RJHW/

Completed : 7-VI-1985
Ordernumber: 543.501
Typ. : MM

FATIGUE FRACTURE IN STEEL LANDING GEAR COMPONENTS

R.J.H. Wanhill
National Aerospace Laboratory NLR
P.O. Box 153, 8300 AD Emmeloord, The Netherlands
Telephone 09-31-5274-2828

SUMMARY

The characteristics of fatigue and overload fracture in high strength low alloy steel landing gear forgings were investigated. Fatigue fracture was characterized by microserrated acicular ridges (misars) and to a lesser extent by striation marks. Overload fracture was by microvoid coalescence (dimples). After corrosion due to outdoor exposure it was still possible to identify fatigue fracture but overload dimples were much less evident. Constant amplitude and block programme (flight-by-flight) fatigue crack propagation rates were well correlated by root mean values of the stress intensity factor range, ΔK_{rm}. This is encouraging for analytical estimation of service failure crack propagation lives.

INTRODUCTION

Aircraft landing gears consist mostly of highly loaded nonredundant components with severe constraints on weight and space. For these reasons many components are made from high strength low alloy steels. During manufacture much effort is made to ensure defect-free components. Nevertheless, undetectable damage or material defects may be present. Also, service operation can result in mechanically and environmentally induced damage.

Fatigue cracks may initiate from the various kinds of damage or defects. Once initiated the fatigue cracks usually propagate to cause component failure, since stresses are high and there is little or no redundancy. In turn, component failure may lead to operational failure of the entire landing gear.

Operational failure is accompanied by much mechanical damage and additional component failures due to overload. Failure investigation must therefore distinguish between fatigue and overload failures. For high strength steels this is by no means an easy task, for three reasons:

1. The types of fracture occurring in fatigue may not be unambiguously relatable to fatigue. Examples are intergranular fracture and microvoid coalescence, which can also occur during overload failure.

2. Features characteristic of fatigue fracture may be partially or completely obliterated by environmental attack (rusting, hydraulic fluid) and mechanical damage during operational failure.

3. The amount of fatigue fracture before component failure is often very limited, since stresses are high and fracture toughnesses relatively low.

With the foregoing considerations in mind the test programme outlined in table 1 was carried out. The main purpose of this programme was to provide guidelines for distinguishing between fatigue and overload failures of high strength steel landing gear components. For this purpose constant amplitude fatigue loading was judged to be most suitable. However, since estimates of fatigue crack propagation lives for service failures are frequently desired, the feasibility of doing this both fractographically and analytically was checked by including tests with approximate flight-by-flight loading.

Table 1. Test programme overview

• MATERIALS	D6AC, 4330V, 300M steel forgings
• SPECIMENS	Standard compact-type (CT)
• FATIGUE LOADINGS	1. Constant amplitude 2. Block programme flight-by-flight
• ENVIRONMENTS	1. Fatigue in laboratory air 2. Outdoor exposure of fracture surfaces
• EXAMINATION	Fractography and metallography
• OBJECTIVES	1. Characterization of fatigue fracture 2. Characterization of overload fracture 3. Influence of exposure on fracture surface appearance 4. Fractographic and metallographic correlations 5. Detection of flight-by-flight fracture surface markings 6. Correlation of fatigue crack growth rates under constant amplitude and flight-by-flight loading

MATERIALS AND SPECIMENS

The materials were D6AC, 4330V and 300M low alloy steel forgings from a main landing gear, figure 1.

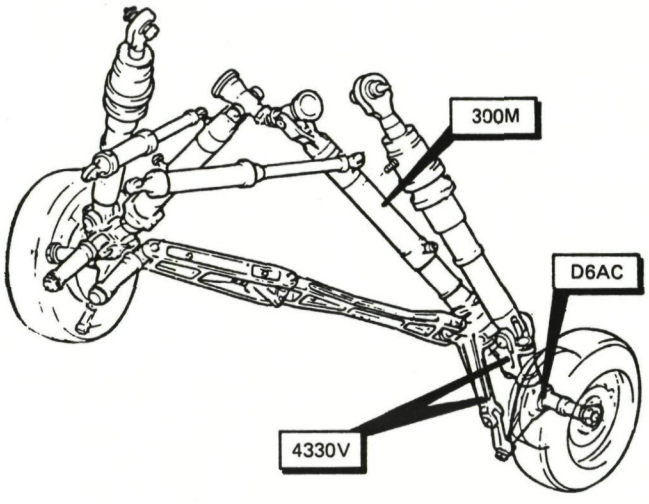

Fig. 1 Main landing gear

Chevron notched compact-type (CT) specimens according to ASTM standard E647 were machined from the forgings before heat treatment. All specimens were oriented with the loading direction parallel to principal loading directions in the original components. The specimens were heat treated according to MIL-H-6875 into the following ranges of ultimate tensile strength: D6AC and 4330V (1517-1655 MPa), 300M (1860-1931 MPa). These strength ranges correspond to those required for the original components.

At this point it may be helpful to discuss briefly the selection of steels and strength levels. 300M is widely used in landing gear components requiring high tensile strength, e.g. the tension strut shown in figure 1. The achievable strength range enables this material to give the highest strength/weight ratio of any commercially available low alloy steel suitable for landing gear.

When other factors such as stiffness and thickness control the design of components it is possible to use lower strength ranges without weight penalties. The selection of a steel then depends on secondary but important considerations. For example, D6AC is deeply hardenable and suitable for heavy sections. It is also heat resistant, which is an advantage for axles (local heating from braking). On the other hand, 4330V is easier to forge into complex shapes, two of which are indicated in figure 1.

EXPERIMENTAL PROCEDURE

The CT specimens were fatigued in laboratory air at room temperature. There were two kinds of fatigue loading:

1. Constant amplitude with load ratio R = P_{min}/P_{max} of 0.1 and cycle frequency 66-150 Hz.

2. Block programme tests approximating flight-by-flight loading with a nominal cycle frequency of 25 Hz.

The block programme is shown in figure 2. It is a simplified version of the load histories developed in references 1 and 2.

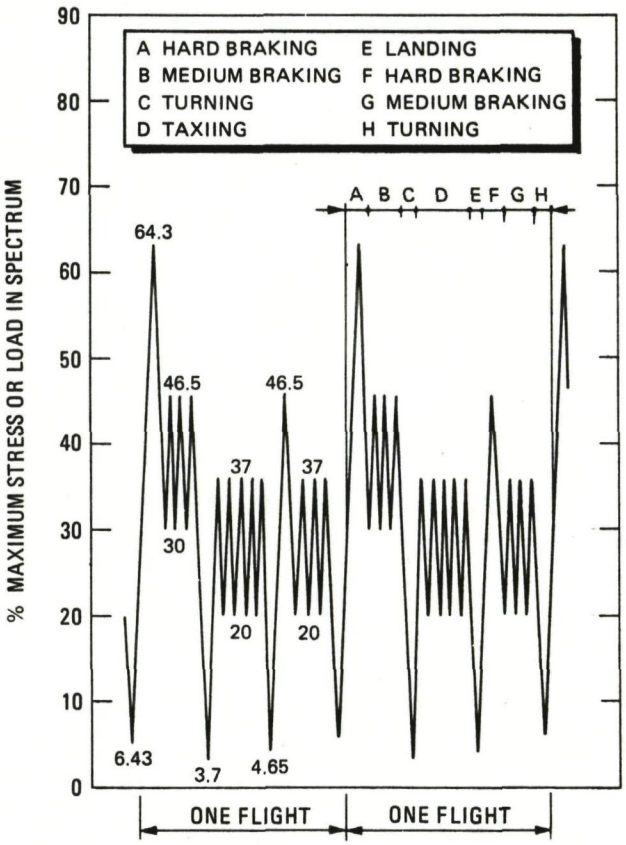

Fig. 2 Block programme approximation of flight-by-flight loading for landing gear components

Crack growth was measured optically. After testing the specimens were broken open. One half of each specimen was examined fractographically and metallographically in the as-tested condition. The remaining halves were exposed outdoors for 100 hours before examination. During this period the weather conditions included temperatures between 265-285K and intermittent precipitation, mostly rain. The fracture surfaces exhibited extensive rust spotting with apparently clean areas in between.

CRACK PROPAGATION RATES

Fatigue crack propagation rates were obtained from increments of crack growth:

$$\frac{da}{dn} = \frac{a_{i+1} - a_i}{n_{i+1} - n_i} \qquad (1)$$

and were correlated with $a^* = (a_{i+1}+a_i)/2$, which corresponds to the mean of the growth interval. Stress intensity factors were calculated from the standard expressions in ASTM Standard E647. Root mean (rm) stress intensity factor ranges were used to correlate the constant amplitude and block

programme data. The general expression for ΔK_{rm} is

$$\Delta K_{rm} = \sqrt[m]{\frac{\Sigma(\Delta K_i)^m n_i}{\Sigma n_i}} \qquad (2)$$

where n_i is the number of load amplitudes corresponding to ΔK_i and m is the slope of the constant amplitude da/dn versus ΔK plot. To derive correct values of ΔK_{rm} it is necessary to account for crack closure. The procedure is discussed in the appendix. Note that when m = 2 one obtains the root mean square value ΔK_{rms}. This has been used for correlating constant amplitude and random load data, e.g. reference 3.

Constant Amplitude Data Correlation

The data are presented in figure 3 together with data envelopes for many steels in two ranges of yield strength[4]. The present results fall within the lower envelope and there is little difference in crack growth rates. For D6AC and 4330V this is not surprising, since the heat treatments resulted in nominal yield strengths of 1300-1350 MPa. However, for 300M the nominal yield strength was at least 1600 MPa, so that significantly higher crack growth rates were expected.

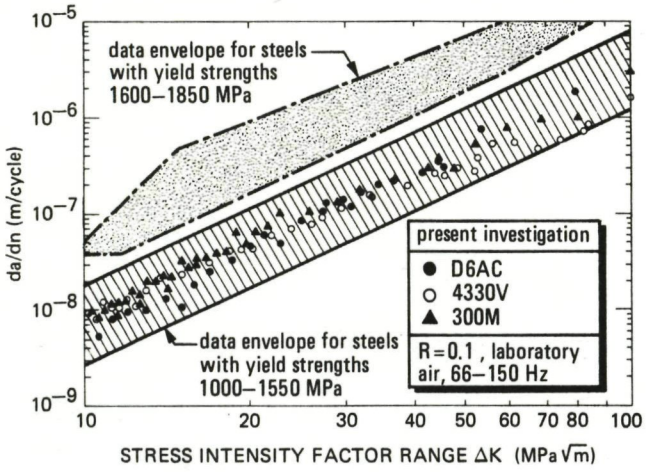

Fig. 3 Constant amplitude fatigue crack growth data

The present data were well represented by the "Paris Law" with the parameters given in table 2. The m values are particularly relevant. It has been shown that m values ≤ 3 imply better fracture toughness and absence of static (i.e. monotonic rather than cyclic) fracture during fatigue[5].

Table 2. "Paris Law" fits to the constant amplitude data

$$\left(\frac{da}{dn}\right)_{R = 0.1} = C(\Delta K)^m$$

	ΔK RANGE (Mpa√m)	C	m
D6AC	10 - 100	7.18×10^{-12}	2.86
4330V	10 - 100	5.49×10^{-11}	2.20
300M	10 - 20	6.75×10^{-12}	3.04
	20 - 100	9.14×10^{-11}	2.17

Block Programme and Constant Amplitude Data Correlation

Crack propagation data for block programme loading were well correlated by ΔK_{rm}, figure 4. Also the correlation of constant amplitude and block programme data by ΔK_{rm} was good, figure 5.

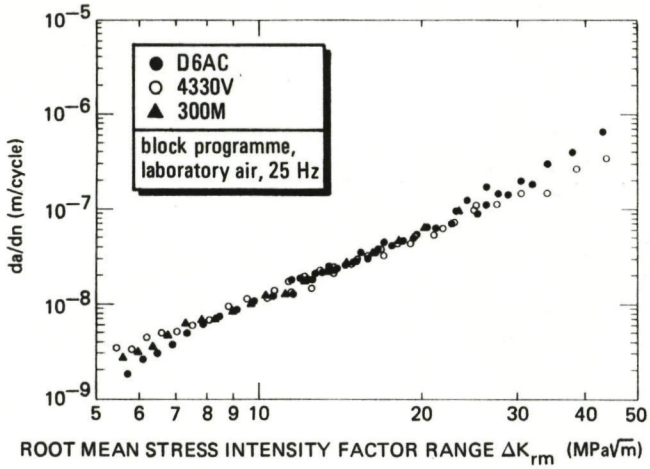

Fig. 4 Block programme fatigue crack growth data

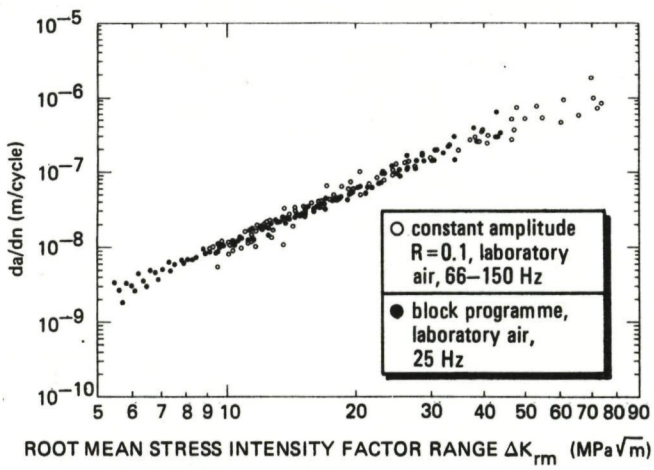

Fig. 5 Correlation of constant amplitude and block programme fatigue crack growth data by ΔK_{rm}

FRACTOGRAPHIC EXAMINATION

Fatigue Fracture

The fatigue fracture surfaces were examined by scanning electron microscopy at several ΔK_{rm} levels. The fractographic appearances were very similar for all three steels under the same type of loading at each ΔK_{rm} level. Also, the fractographic appearances at lower magnifications ($\leq$ 1000X) were similar when ΔK_{rm} for constant amplitude loading was about twice that for block programme loading.

Examples are given in figure 6. In more detail the following trends were observed.

1. For ΔK_{rm} values of 6 MPa$\sqrt{m}$ (block programme) and 10 MPa$\sqrt{m}$ (constant amplitude) the fatigue fracture surfaces consisted mainly of microserrated acicular ridges (misars) with isolated intergranular facets. Fatigue striations were not resolvable.

2. For ΔK_{rm} values of 10 MPa$\sqrt{m}$ (block programme) and 20 MPa$\sqrt{m}$ (constant amplitude) examination at higher magnification revealed subtle "rounding" of the misars, most probably owing to increased crack tip plasticity, and fatigue striation marks on fracture surfaces produced during block programme loading. These are illustrated in the middle column/bottom row of figure 6.

3. For ΔK_{rm} values of 20 MPa$\sqrt{m}$ (block programme) and 40 MPa$\sqrt{m}$ (constant amplitude) the typical misar appearance was no longer identifiable, but striations were visible on fracture surfaces produced during both constant amplitude and block programme loading. However, the striations were often irregular, which detracts from their diagnostic usefulness since they then resemble stretch and tear markings.
The fatigue striation marks for block programme loading were wider than those for constant amplitude loading although, as may be ascertained from figure 5, the cyclic crack growth rate was lower. The explanation is that the fatigue striation marks for block programme loading represented flight blocks, not individual cycles. This is also the reason why striation marks at lower ΔK_{rm} values were visible only for block programme loading.

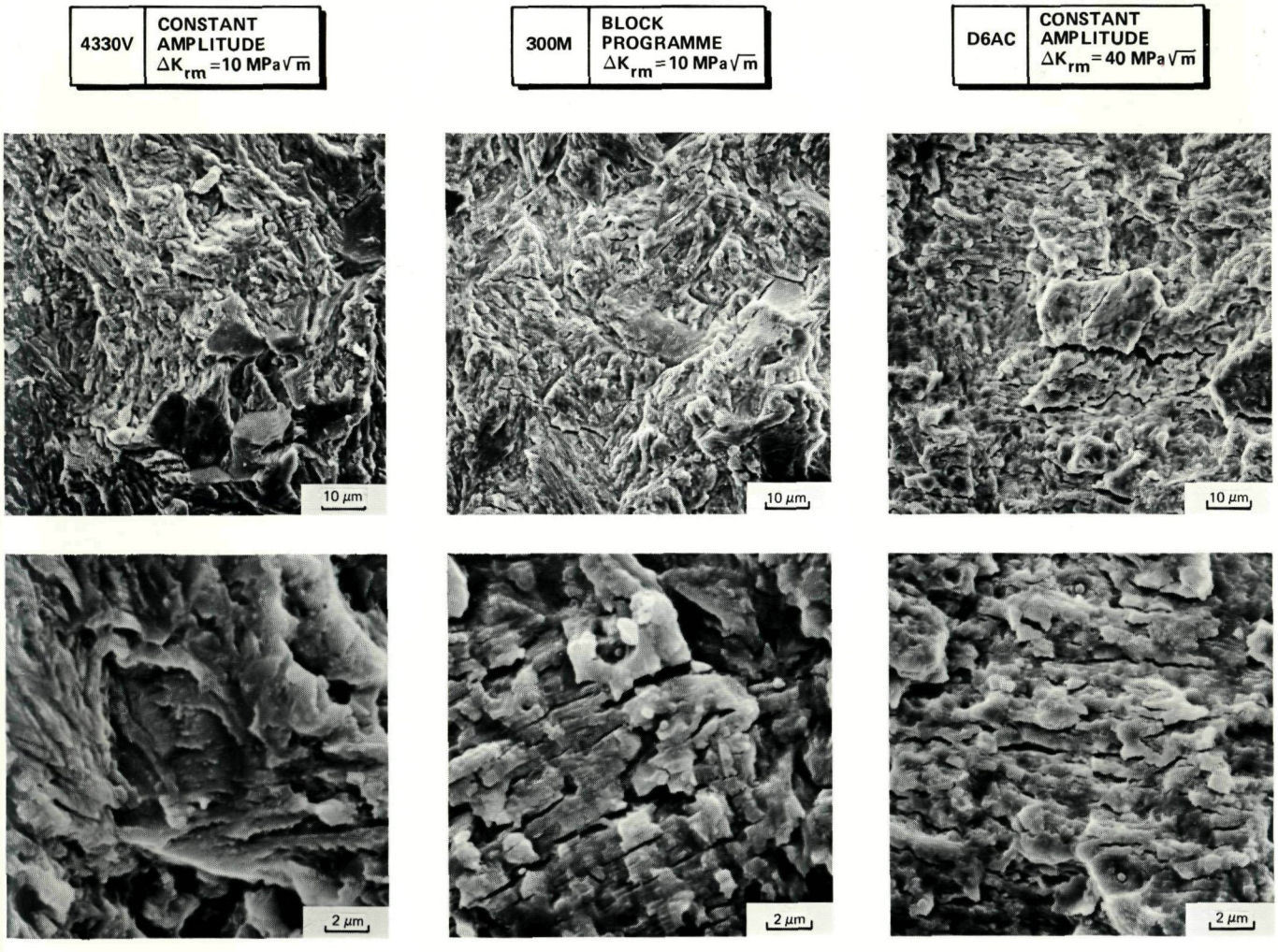

Fig. 6 Examples of fatigue fracture characteristics for all three steels

4. Outdoor exposure resulted in extensive but discontinuous corrosion (rusting) with fairly clean areas in between. In these clean areas misars, intergranular facets and fatigue striations were identifiable, particularly the misars.

Overload Fracture

For all three steels the overload fracture surfaces were covered by a mixture of small and large dimples formed by microvoid coalescence. This is a very distinctive type of fracture. However, outdoor exposure made it far less evident, as can be seen in figure 7.

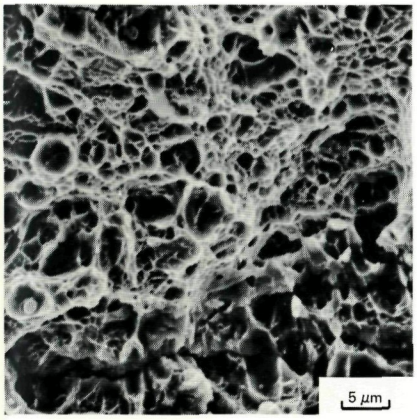

4330V
AS FRACTURED

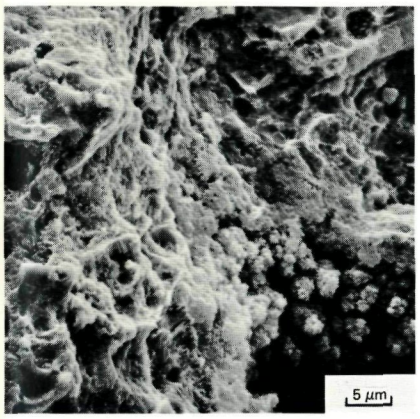

D6AC
AFTER OUTDOOR
EXPOSURE

Fig. 7 Examples of overload fracture characteristics

METALLOGRAPHIC AND FRACTOGRAPHIC CORRELATIONS

Metallographic sections parallel to the macroscopic plane of fracture were prepared by standard techniques. All three steels had similar microstructures of tempered martensite needles with evidence of prior austenite grain boundaries. There were two fracture features that could be related directly to the microstructures:

1. The microserrated acicular ridges (misars) which had sizes and aspect ratios similar to those of the tempered martensite needles.

2. Isolated intergranular facets, corresponding to prior austenite grain boundaries.

Examples of the similarity of misars and tempered martensite needles, and hence most probably their correspondence, are given in figure 8.

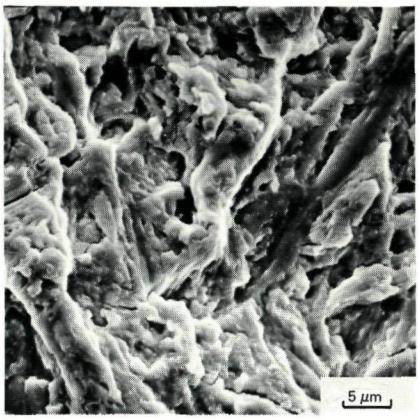

FRACTOGRAPH

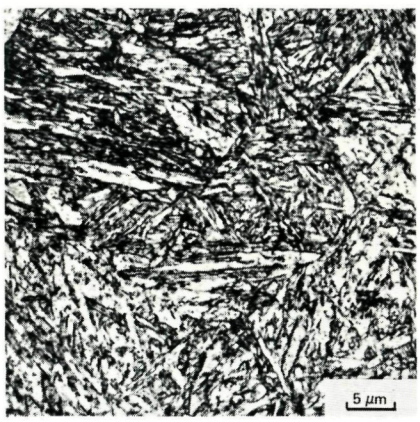

METALLOGRAPH

Fig. 8 Example of similar morphology of misars and tempered martensite needles: 4330V steel

DISCUSSION

Fatigue fracture was characterized by microserrated acicular ridges (misars) and striation marks, which were particularly visible for block programme (flight-by-flight) loading. The striations were often irregular, which detracts from their diagnostic usefulness.

In the absence of corrosion the fatigue fractures were clearly distinguishable from overload fracture, which occurred by microvoid coalescence. However, after outdoor exposure resulting in extensive rust spotting the characteristic dimples of overload fracture were far less evident. Distinguishing between fatigue and overload fracture then relies mainly on identifying fatigue from misars and striation marks in locally cleaner areas.

Misars are especially useful for identifying fatigue fractures in high strength low alloy steels. They are readily visible by scanning electron microscopy and occur widely. This is most probably because they represent cyclic deformation and fracture influenced locally by the presence of

tempered martensite needles characteristic of the microstructures of such steels.

Constant amplitude and block programme fatigue crack propagation rates were well correlated by root mean values of the stress intensity factor range, ΔK_{rm}. This is encouraging for analytical estimation of service failure crack propagation lives when the load history is known or can be estimated and contains peak loads with a short recurrence period, e.g. once per flight. In view of the difficulty in observing regular fatigue striations, particularly for lower ΔK_{rm} values, it is unlikely that fractography (striation counting) will provide good estimates of service failure crack growth lives. However, fractography can assist in the derivation of appropriate values of ΔK_{rm}, see the appendix.

Finally, the fact that fatigue fracture appearances at lower magnifications were similar when ΔK_{rm} for constant amplitude loading was about twice that for block programme loading can be explained as follows. The overall appearances of the fatigue fractures were probably controlled by the maximum extent of cyclic plasticity in the crack tip region. For constant amplitude loading the maximum extent of the cyclic plasticity is simply related to ΔK_{rm} via an expression for the cyclic plastic zone size. However, for block programme loading the maximum extent of crack tip cyclic plasticity is determined by the largest load excursion per flight block. Accounting for crack closure (see the appendix) ΔK_{eff} of the largest load excursion is approximately twice ΔK_{rm} for the flight block: hence the foregoing similarity.

CONCLUSIONS

An investigation of fatigue and overload fracture in high strength low alloy steel landing gear forgings has shown the following:

1. Fatigue fracture was characterized by microserrated acicular ridges (misars) and to a lesser extent by striation marks, which were more evident for block programme (flight-by-flight) loading.

2. The overall appearances of fatigue fractures were probably controlled by the maximum extent of crack tip cyclic plasticity, which in the case of block programme loading is determined by the largest load excursion per flight block.

3. Uncorroded fatigue and overload fractures could readily be distinguished. Overload occurred by microvoid coalescence resulting in well-defined dimples.

4. After outdoor exposure resulting in extensive rust spotting the dimples characterizing overload fracture were far less evident. Distinguishing between fatigue and overload fractures then has to rely mainly on identifying fatigue from misars and striation marks.

5. Misars and intergranular facets on fatigue fracture surfaces correlated with the tempered martensite needles and prior austenite grain boundaries in the microstructures.

6. Constant amplitude and block programme fatigue crack propagation rates were well correlated by root mean values of the stress intensity factor range, ΔK_{rm}.

7. Correlation of fatigue crack propagation rates by ΔK_{rm} is encouraging for analytical estimation of service failure crack growth lives.

8. Since regular fatigue striations were infrequent it is unlikely that fractography will provide good estimates of service failure fatigue crack growth lives.

ACKNOWLEDGEMENT

This investigation was carried out under contract with the Scientific Research Division of the Directorate of Materiel, Royal Netherlands Air Force.

REFERENCES

1. H.D. Dill and C.R. Saff, "Environment-load interaction effects on crack growth", Air Force Flight Dynamics Laboratory Report AFFDL-TR-78-137, November 1978.

2. C.R. Saff, "Environment-load interaction effects on crack growth in landing gear steels", Naval Air Development Centre Report NADC-79095-60, December 1980.

3. J.M. Barsom, "Fatigue crack growth under variable-amplitude loading in various bridge steels", Fatigue Crack Growth Under Spectrum Loads, ASTM STP 595, pp. 217-235 (1976): Philadelphia.

4. R.J.H. Wanhill, "Microstructural influences on fatigue and fracture resistance in high strength structural materials", Engineering Fracture Mechanics, Vol. 10, pp. 337-357 (1978).

5. R.O. Ritchie and J.F. Knott, "Mechanisms of fatigue crack growth in low alloy steel", Acta Metallurgica, Vol. 21, pp. 639-648 (1973).

6. A.U. de Koning, "Crack growth prediction methods", NLR Report TR 84121 L, December 1984.

7. G.M. van Dijk, "Statistical load data processing", Advanced Approaches to Fatigue Evaluation, NASA SP-309, pp. 565-598 (1972).

8. M. Matsuiski and T. Endo, "Fatigue of metals subjected to varying stress", Kyushu District Meeting of the Japan Society of Mechanical Engineers, March 1968.

9. R. Sunder, S.A. Seetharam and T.A. Bhaskaran, "Cycle counting for fatigue crack growth analysis", International Journal of Fatigue, Vol. 6, pp. 147-156 (1984).

10. W. Elber, "Equivalent constant-amplitude concept for crack growth under spectrum loading", Fatigue Crack Growth Under Spectrum Loads, ASTM STP 595, pp. 236-250 (1976): Philadelphia.

11. G. Glinka, C. Robin, G. Pluvinage and C. Chehimi, "A cumulative model of fatigue crack growth and the crack closure effect", International Journal of Fatigue, Vol. 6, pp. 37-47 (1984)

APPENDIX: CORRELATION OF BLOCK PROGRAMME AND CONSTANT AMPLITUDE DATA BY ΔK_{rm}

INTRODUCTION

For some types of variable amplitude load history fatigue crack growth is a regular process because peak loads have either a short recurrence period or only minor effects on crack extension in subsequent load excursions. In such cases it is often possible to correlate crack growth rates using a characteristic stress intensity factor, e.g. reference 3.

One possibility, used in the present paper to correlate block programme and constant amplitude data, is the root mean value of the stress intensity factor range, ΔK_{rm}.

The general expression for ΔK_{rm} is

$$\Delta K_{rm} = \sqrt[m]{\frac{\Sigma(\Delta K_i)^m n_i}{\Sigma n_i}} \qquad (A1)$$

where n_i is the number of load amplitudes corresponding to ΔK_i and m is the slope of the constant amplitude da/dn versus ΔK plot. The main problem in the use of equation (A1) is the derivation of ΔK_i values. To do this properly it is necessary to account for crack closure and follow a rational procedure of cycle counting.

DETERMINATION OF ΔK_i

Consider the load histories shown in figure A1 and expressed in terms of stress intensity factors.

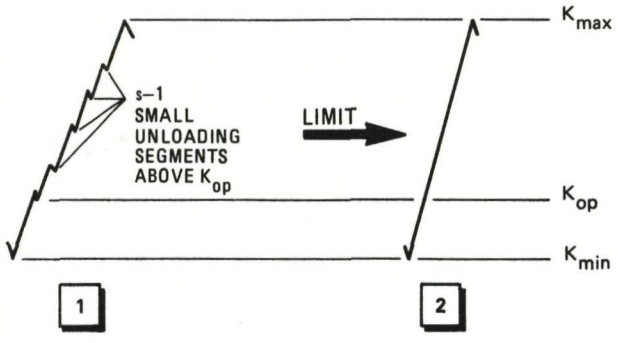

Fig. A1 Similar load histories expressed in terms of K

Using the Elber relation $da/dn = C(\Delta K_{eff})^m$ the crack growth increment for load history [1], which consists of s uploading segments, is given by

$$\Delta a = sC \frac{K_{max} - K_{op}}{s}^m \qquad (A2)$$

For load history [2]

$$\Delta a = C(K_{max} - K_{op})^m \qquad (A3)$$

In general the crack growth increments given by equations (A2) and (A3) will be different, although the load histories are similar and in the limit identical. This means that a crack growth "law" cannot be applied straightforwardly to parts of load cycles or to load histories like [1].

To solve this problem De Koning[6] proposed integration of the incremental form of the crack growth law. Using the Elber relation one then obtains for each segment s of load history [1]:

$$\left.\begin{aligned} \Delta a_s &= C[(K_{max_s} - K_{op})^m - (K_{min_s} - K_{op})^m] \\ &\qquad \text{for } K_{op} < K_{min_s} \\ &= C[K_{max_s} - K_{op})^m] \text{ for } K_{op} \geq K_{min_s} \end{aligned}\right\} \qquad (A4)$$

Use of equations (A4) enables correct estimation of the crack growth contribution by small load excursions. Support for this assertion is provided by the compatibility of equations (A4) with the successful method of cycle counting known as range pair-range[7] or "rainflow"[8]. This will be illustrated by figure A2, which shows two load histories that give identical crack growth increments according to rainflow cycle counting[9].

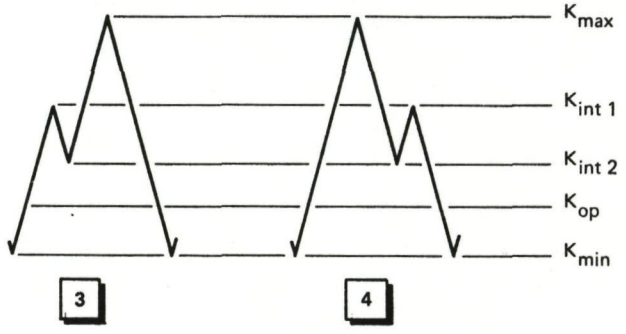

Fig. A2 Two load histories with identical crack extension according to rainflow cycle counting

From equations (A4) the crack growth increments for load histories [3] and [4] are given by

$$\Delta a_3 = C[(K_{int_1} - K_{op})^m + (K_{max} - K_{op})^m - (K_{int_2} - K_{op})^m]$$

$$\Delta a_4 = C[(K_{max} - K_{op})^m + (K_{int_1} - K_{op})^m - (K_{int_2} - K_{op})^m]$$

which are identical.

Now consider the load history shown in figure A3 and containing a small load excursion [i]. The

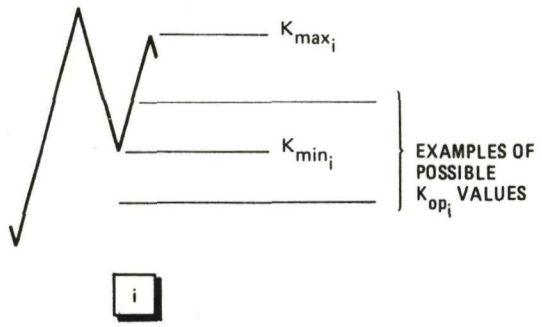

Fig. A3 A small load excursion expressed in terms of K

crack growth increment for load excursion [i] is given by

$$\Delta a_i = C(\Delta K_i)^m$$

where

$$(\Delta K_i)^m = (K_{max_i} - K_{op_i})^m - (K_{min_i} - K_{op_i})^m \quad \text{for } K_{op_i} < K_{min_i}$$

$$= (K_{max_i} - K_{op_i})^m \quad \text{for } K_{op_i} \geq K_{min_i} \qquad \text{(A5)}$$

DETERMINATION OF K_{op_i}

Equations (A5) require estimates of K_{op_i}. It is obviously possible to obtain some kind of record of crack opening and closing during fatigue testing. However, such measurements may be difficult to interpret, they may have been omitted, or else only service failures have occurred under the load history of interest. In such cases it may be possible to obtain reasonable estimates of K_{op_i} from examination of the fatigue fracture surfaces. This will be discussed next.

Fractographic Estimation of K_{op_i}

For a fractographic estimate of K_{op_i} to be possible there are several requirements:

1. The load history must be variable amplitude.

2. The load history should be known and fairly simple, or else should contain recognisable sequences whose load levels can be estimated.

3. Fatigue fracture surfaces must show striation patterns.

4. The crack opening stress or load from which K_{op_i} is derived should be effectively constant.

5. The value of m should be known or can be estimated.

Requirement (4) might seem very restrictive, but it is reasonable for load histories in which peak loads have a short recurrence period or only minor effects on crack extension in subsequent load excursions, e.g. reference 10.

The procedure for estimating K_{op_i} for the block programme loading used in the present investigation is as follows. Consider the loading pattern for one block of the flight-by-flight sequence, figure A4. The load block can be considered in terms of thirteen increasing-K segments that contribute to fatigue crack growth.

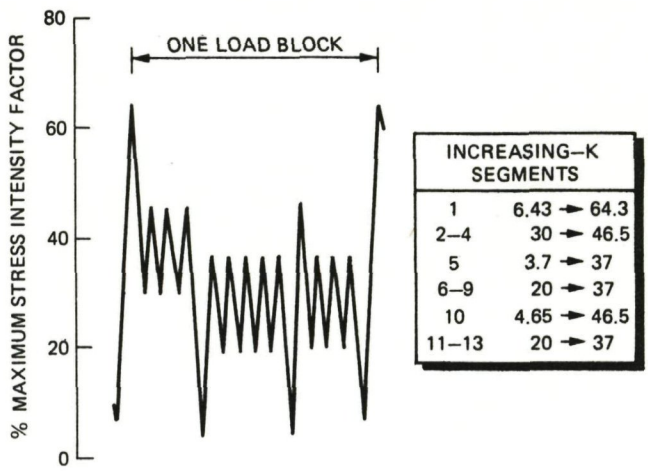

Fig. A4 A load block from the sequence used in the present investigation

The following steps have to be carried out:

- choice of material and hence m
- choice of several hypothetical K_{op_i} levels
- calculation of relative spacings of fatigue striations produced during each increasing-K segment, using equations (A5)

- comparison of actual and calculated relative spacings of fatigue striations to obtain a best fit and hence an estimate of K_{op_i}.

An example of the results of the first three steps is shown in figure A5 and table A1. Note that the changes in relative striation spacings with changing K_{op_i} are subtle. In fact, it is essential to calculate relative striation spacings for a number of K_{op_i} levels before examining actual fracture surfaces in detail.

Table A1. Predicted relative spacings of fatigue striations for 4330V steel: m = 2.20

K_{op_i} (% maximum)	Increasing-K segments for one load block					
	1	2-4	5	6-9	10	11-13
0	1	0.307	0.296	0.229	0.490	0.229
10	1	0.306	0.215	0.191	0.417	0.191
15	1	0.300	0.168	0.162	0.373	0.162
20	1	0.285	0.122	0.122	0.323	0.122
25	1	0.255	0.074	0.074	0.265	0.074
30	1	0.200	0.030	0.030	0.200	0.030

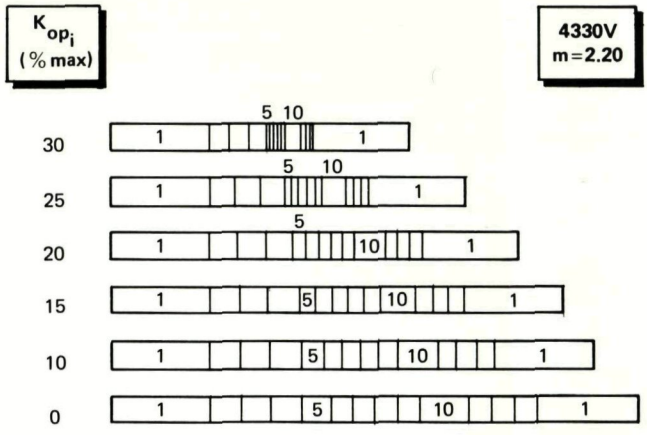

Fig. A5 Predicted relative spacings of fatigue striations for 4330V steel subjected to block programme loading. Increasing-K segments 1,5 and 10 are indicated

Estimation of K_{op_i} for the Present Investigation

No crack closure records were available from the tests discussed in the main body of this paper. For constant amplitude tests of a high strength steel at R = 0.1 a reliable estimate of K_{op_i} is

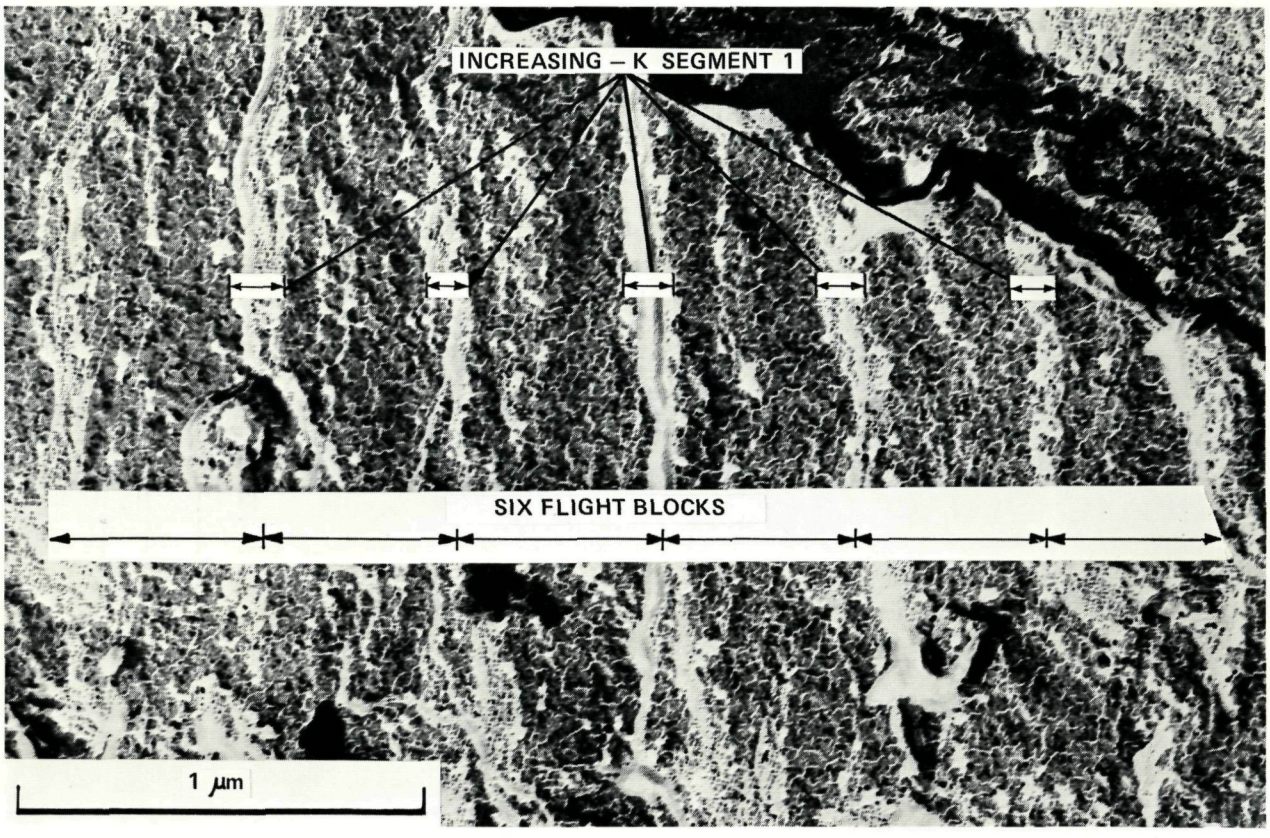

Fig. A6 Fatigue striation marks for block programme loaded 4330V steel at $\Delta K_{rm} \sim 18$ MPa $\sqrt{m}$: transmission electron fractograph of a two-stage replica, 0^{o} tilt

given in reference 11. It was found that $\Delta K_{eff}/\Delta K = 0.9$ over a wide range of ΔK. Thus for the constant amplitude tests in the present investigation ΔK_{rm} was taken to be 0.9 ΔK in order to account for crack closure.

For block programme loading tests there were two possibilities to estimate K_{op_i}. First, an extensive series of crack opening displacement measurements for 7075-T651 aluminium alloy showed K_{op_i} to be approximately constant at 17 % of the maximum stress intensity factor. Second, K_{op_i} was estimated from fractographs. For this purpose 4330V specimens were examined because this steel had the lowest m value and was therefore expected to most clearly indicate fatigue striations for all of the increasing-K segments. However, even at very high magnifications it was possible to identify only the flight blocks and the largest striations corresponding to increasing-K segment 1, e.g. figure A6.

On average the largest striations accounted for slightly less than 30 % of the flight block widths. The corresponding K_{op_i} value was close to that for 7075-T651. Thus a K_{op_i} value of 17 % of the maximum stress intensity factor (see figure A4) was used to calculate ΔK_i and hence ΔK_{rm} for the steels tested in the present investigation under block programme loading. This resulted in good correlation of the block programme and constant amplitude crack growth data by ΔK_{rm}, as is shown in figure 5 in the main body of this paper.

NATIONAAL LUCHT- EN RUIMTEVAARTLABORATORIUM

Anthony Fokkerweg 2, 1059 CM AMSTERDAM
Postbus 90502 , 1006 BM AMSTERDAM
Tel. (020) 5113113 - telex 11118 (nlraa nl)
Telegram-adres: Windtunnel Amsterdam